Molecular Self-Assembly on Ultrathin Metallic Surfaces: Alkanethiolate Monolayers on Ag(1 × 1)−Au(111)

M. Fonticelli,[†] O. Azzaroni,[†] G. Benítez,[†] M. E. Martins,[†] P. Carro,[‡] and R. C. Salvarezza*[,†]

Instituto de Investigaciones Fisicoquímicas Teóricas y Aplicadas (INIFTA), Universidad Nacional de La Plata−CONICET, Sucursal 4 Casilla de Correo 16 (1900) La Plata, Argentina, and Departamento de Química Física, Universidad de La Laguna, Tenerife, Spain

Received: July 4, 2003; In Final Form: October 31, 2003

The self-assembly of alkanethiols on underpotentially deposited Ag(1 × 1)−Au(111) has been studied by using scanning tunneling microscopy, Auger electron spectroscopy, and electrochemical techniques. Even for short adsorbed alkanethiolates, the surface structure consists of an incommensurate hexagonal lattice with nearest-neighbor distances ≈ 0.48 nm that are usually found for long alkanethiolates adsorbed on the Ag(111) surface. Surprisingly, the stability of the self-assembled alkanethiolate monolayers against reductive electrodesorption is increased in ∼0.10 and 0.40 V with respect to those observed on Ag(111) and Au(111), respectively. Density-functional theory calculations for methanethiolate desorption from a model cluster indicate that the enhanced stability arises from a balance between the energy to introduce an electron into the alkanethiolate−Ag(1 × 1)−Au(111) system and the alkanethiolate desorption energy that is strongly modified by the Au substrate.

1. Introduction

Ultrathin metallic films, one atomic layer in thickness, are of special interest due to their unique catalytic and chemisorptive properties.[1] In particular, it is of great interest to know if a metal monolayer (overlayer) on a foreign substrate exhibits an anomalous chemisorption behavior in relation to the respective bulk metal.[2] In fact, the study of molecular chemisorption on this type of system could allow us to elucidate the interplay between surface electronic structure and reactivity of transition and noble metals,[3] a matter that is still far from a complete understanding. The development of density-functional theory (DFT) combined with accurate experimental data has emerged new possibilities for the study of chemisorption on metal surfaces. In this way, a systematic study based on DFT calculations and experimental data has been done for CO adsorption on metal overlayers supported on transition and noble metals substrates[2,3] in order to understand the physicochemical factors[4] ruling this type of system.

Alkanethiol chemisorption on noble metals leading to self-assembled monolayers (SAMs) has attracted considerable scientific interest.[5a] SAMs provide a route to control corrosion, wetting, and wear properties of metal surfaces, they serve to anchor different functional groups used as chemical and biochemical sensors,[5a] they are used to fabricate nano-devices for electronics,[6] they are promising candidates for new nano-fabrication methods,[7] and finally they are ideal model systems for interface science.[8]

It is well known that the Au(111)−alkanethiolate surface consists of an ordered ($\sqrt{3} \times \sqrt{3}$)R30° lattice[5a] and its related c(4 × 2) superlattice, both in the gaseous[9a] and liquid[9b] environments. The alkanethiolate molecules in these lattices are chemisorbed on the Au surface by the S heads, forming a thiolate bond.[5a,10] The hydrocarbon chain presents a tilt angle ranging from 20 to 40° with respect to the substrate normal.[11] The ($\sqrt{3} \times \sqrt{3}$)R30° lattice exhibits nearest-neighbor distances $d \approx 0.5$ nm,[5a] while the c(4 × 2) lattice exhibits some pairing of the S atoms as revealed by grazing-incidence X-ray diffraction (GIXD) data.[8] Scanning tunneling microscopy (STM) measurements have shown $d = 0.45$ nm between the bright and dark spots (inter-row distance) and $d = 0.5$ nm inside the row (intrarow distance) of the c(4 × 2) superlattices.[9b] In the case of alkanethiolate adsorption on Ag(111), chemisorbed molecules are also bonded by the S head to the Ag surface, although their tilt angles with respect to the substrate normal range from 0 to 15°.[12a] Previous STM studies have shown that alkanethiolates with long hydrocarbon chains organize on Ag(111), forming slightly distorted incommensurate hexagonal adlayers with $d = 0.46-0.48$ nm,[12b] that is expanded with respect to the $d = 0.44$ nm found in the ($\sqrt{7} \times \sqrt{7}$)R19.1° lattice observed for S and short alkanethiols on Ag(111).[13,14] It has been reported that the S head of the alkanethiolate species in the ($\sqrt{7} \times \sqrt{7}$)-R19.1° lattice are placed at hollow and top sites. The value $d = 0.46-0.48$ nm has also been observed in close-packed bulk alkanes.[5a]

The self-assembly of these two-dimensional structures implies alkanethiolate−metal, alkanethiolate−alkanethiolate, alkanethiolate−environment, and metal−environment interactions. In the case of electrolyte solutions, reductive electrodesorption curves have been used to estimate these contributions.[15] In fact, Au(111) ($\sqrt{3} \times \sqrt{3}$)R30° and c(4 × 2) and Ag(111) ($\sqrt{7} \times \sqrt{7}$)R19.1° alkanethiolate lattices are desorbed in sharp voltammetric peaks according to this reaction

$$(CH_3)(CH_2)_nS-Me + solvent + e = [(CH_3)(CH_2)_nS^-]_{solv} + Me_{solv} \quad (1)$$

In eq 1, $(CH_3)(CH_2)_nS-ME$ stands for the adsorbed alkanethiolatespecies on the Me substrate, $[(CH_3)(CH_2)_nS^-]_{solv}$ for

* Author to whom correspondence may be addressed. E-mail: robsalva@inifta.unlp.edu.ar.
[†] Universidad Nacional de La Plata.
[‡] Universidad de La Laguna.

10.1021/jp0359384 CCC: $27.50
Published on Web 01/14/2004

the solvated desorbed alkanethiolate, and Me_{solv} for the solvated substrate. The peak potential shifts in the negative direction as the number of CH_2 units (n) in the hydrocarbon chain of the alkanethiolate molecules increases. On the basis of the peak potential (E_p) vs n plots, the stabilizing interactions in aqueous 0.1 M NaOH solutions (van der Waals + hydrophobic forces) have been estimated in the 3−4 kJ/mol range per methylene unit for both Au(111) and Ag(111) substrates.[15,16] The magnitude of these interactions decreases to 2 kJ/mol per methylene unit in 0.1 M NaOH methanolic solutions.[17,18] It has been also shown that for a constant n, the alkanethiolate molecules are desorbed from Ag(111) at more negative potential values than those corresponding for the desorption from Au(111). This difference has tentatively been explained by the smaller work function value[19] or the stronger Lewis acid behavior of Ag with respect to Au.[20] We have recently demonstrated by DFT calculations that, for a given alkanethiolate (n = cte), the electrodesorption potentials depend on different contributions, the energy to introduce an electron in the alkanethiolate−metal system, the energy to desorb the negatively charged alkanethiolate from the metal surface, and finally the solvation energy of the metal.[21]

It is interesting to note that Ag and Au present many similarities such as they crystallize in the fcc structure, they have almost identical lattice parameters, they have comparable surface free energies, and they are isoeletronic.[22] However, they also present significant differences, the Ag(111) surface does not reconstruct while Au(111) has a complex surface reconstruction and the energy separation of the L gap and the corresponding bulk state is also quite different for Ag(111) and Au(111). As a consequence, while the Au(111) surface states seem to be confined in the surface, the wave functions for Ag(111) will extend longer into the bulk. Besides, the work functions of these metals differs by ∼0.8 eV.

From the above discussion, it appears that alkanethiolate adsorption on a Ag monolayer deposited on a Au(111) substrate is an excellent system for experimental and theoretical studies on alkanethiolate chemisorption on metal overlayers. Two-dimensional structures consisting of a metal on a foreign metallic substrate can easily be prepared by underpotential deposition[23−25] from electrolyte solutions. Depending on the applied potential (E), the surface coverage can be changed from the submonolayer regime to a complete overlayer in a controlled way. Underpotentially deposited (upd) Ag on Au(111) has been the subject of numerous electrochemical studies complemented with in situ STM, atomic force microscopy (AFM), and low-energy electron diffraction.[26,27] All these studies report the formation of a compact Ag(1 × 1)−Au(111) structure at potentials slightly more positive than the reversible potential of the Ag^+/Ag redox couple in the working solution. First-principles calculations have also shown that the Ag(1 × 1)−Au(111) structure is stable while low-coverage Ag phases on the Au(111) surface could be stabilized by anion adsorption induced by the strong modification in the work-function values that produces the Ag adsorbate.[28] It must be remarked that, even though the SAM on the overlayer-modified foreign substrate is easily prepared, only a few studies have been done on this particular system,[29−32] and more important, only a few studies have been carried out on self-assembled organic monolayers chemisorbed on metal upd/foreign substrates systems.[33−35]

In this paper, we have studied the behavior of Ag(1 × 1)-covered Au(111) by following the electrodesorption of alkanethiolate SAMs with $3 \le n \le 12$ in aqueous 0.1 M NaOH. We have tried to answer the following questions: Which is the influence of the metal overlayer and the underlying substrate layers on the adsorbate surface structure? Which is the influence of the overlayer and the substrate on the electrochemical stability of the adsorbate species? How are the electronic states of the adsorbate/metal overlayer influenced by the substrate? How is the adsorption energy of the adsorbate species on the overlayer modified by the foreign substrate? For this purpose, we have used electrochemical techniques, Auger electron spectroscopy (AES), STM, and DFT calculations on cluster models. We have found that even for short alkanethiolate adsorbates the surface structure consists of an incommensurate hexagonal lattice with nearest-neighbor distances ≈ 0.48 nm that are usually found for long alkanethiolates adsorbed on the Ag(111) surface. We also observed that the stability of the SAMs against reductive electrodesorption is increased in ∼0.10 and 0.40 V with respect to those measured on Ag(111) and Au(111), respectively. DFT calculations for methanethiolate desorption from a model cluster indicate that this stability mainly arises from a balance between the energy to introduce an electron into the alkanethiolate-Ag-(1 × 1)−Au(111) system and the alkanethiolate desorption energy.

2. Experimental Section

Evaporated Au and Ag on chromium-coated glass (Arrandee) were used as substrates. After flame annealing in hydrogen atmosphere, their surfaces consist of micrometer-sized grains with atomically smooth (111) terraces separated by monatomic steps as revealed by STM imaging. The Au substrate quality was also tested by cyclic voltammetry in 1 M H_2SO_4. The Ag-(1 × 1)−Au(111) surface was voltammetrically prepared by Ag upd on the Au substrates from 5×10^{-4} Ag_2SO_4 + 1M H_2SO_4 at a scan rate of $\upsilon = 0.01$ V s^{-1}. Voltammetric runs were made in a glass-made electrochemical cell containing three electrodes. A large Pt plate was used as a counterelectrode. Ag^+/Ag, reversible hydrogen, and saturated calomel were used as reference electrodes for Ag upd, Au characterization in 1 M H_2SO_4, and alkanethiolate electrodesorption measurements, respectively. However, in the text, all potential values are referred to the saturated calomel electrode.

Alkanethiolate monolayers were self-assembled on the Au(111), Ag(111), and Ag(1 × 1)−Au(111) surfaces by immersion in ethanolic solution containing 5×10^{-5} M of alkanethiols (immersion time 20 h at room temperature). Alkanethiols with different chain length (n) were used separately, propanethiol, hexanethiol, decanethiol, and dodecanethiol. Surface characterization of the alkanethiolate monolayers was made by using STM (Nanoscope III, Digital Instruments) and AES using a single-pass cylindrical mirror analyzer (CMA, Physical Electronics).

Electrodesorption potentials were measured from cathodic polarization curves recorded at 0.05 V s^{-1} in aqueous 0.1 M NaOH.

3. Results and Discussion

3.1. Preparation and Characterization of the Ag(1 × 1)−Au(111) Surface. Typical current density (j) vs potential (E) profile recorded for the preferred oriented Au(111) substrate in 5×10^{-4} M Ag_2SO_4 + 1 M H_2SO_4 at a scan rate of $\upsilon = 0.01$ V s^{-1} between the anodic limit $E_s = 1.10$ V and the cathodic limit $E_c = 0.42$ V ($E_c > E_r$, E_r is the reversible potential of the Ag/Ag^+ redox couple) is shown in Figure 1. Therefore, the recorded voltammetric response corresponds to the Ag electrodeposition on Au(111) in the underpotential region. The profile exhibits three main features: a sharp and reversible pair

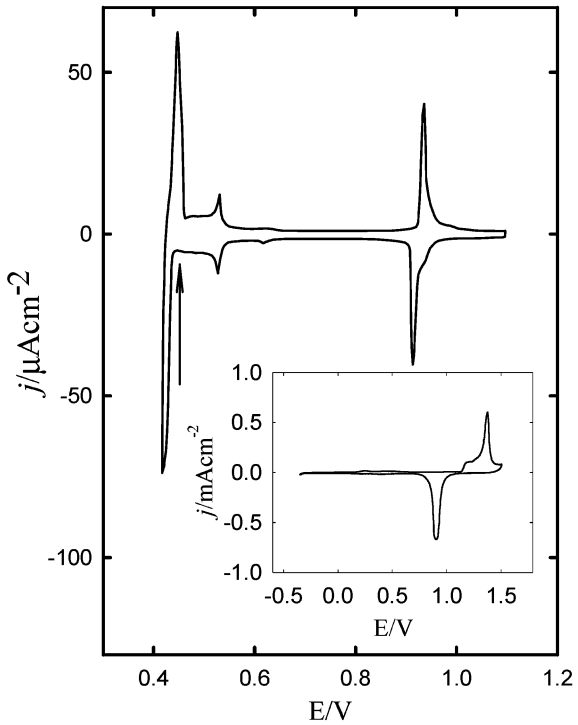

Figure 1. Typical j vs E profile for the Au(111) substrate in 5×10^{-4} M $Ag_2SO_4 + 1$ M H_2SO_4 recorded at a scan rate $\upsilon = 0.01$ V s^{-1} from $E_s = 1.10$ V to $E_c = 0.42$ V. The typical reversible peaks related to the underpotential deposition of two Ag monolayers are shown. The arrow indicates the potential value ($E = 0.45$ V) used to form the Ag-(1×1)−Au(111) surface structure. The inset shows the typical voltammogram of the Au(111) substrate in 1 M H_2SO_4, $\upsilon = 0.10$ V s^{-1}.

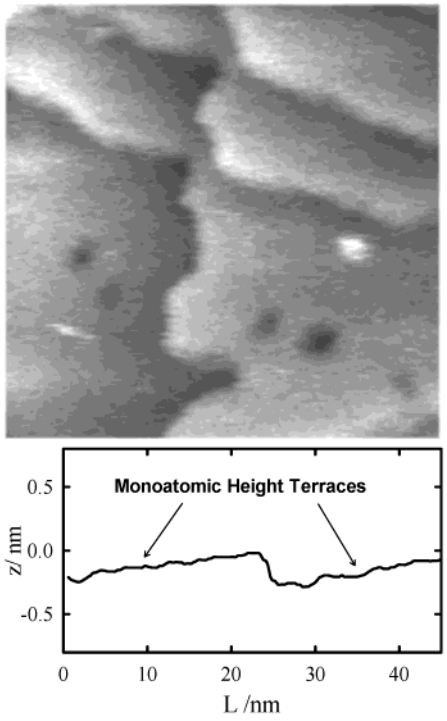

Figure 2. 45×45 nm^2 STM image of the Ag(1×1) monolayer on the Au(111) substrate.

of conjugated peaks at 0.93 V that has been assigned to the formation/stripping of a $(\sqrt{3} \times \sqrt{3})$R30° Ag lattice, a small pair of reversible conjugated peaks at 0.50 V that correspond to the formation/stripping of a denser Ag layer that is completed at 0.45 V leading Ag(1×1)−Au(111),[26,27] and at more negative potentials (slightly positive with respect to E_r) a large and reversible pair of peaks is recorded that is related to the formation/stripping of a second Ag layer on the first Ag monolayer. Thus, to voltammetrically form the Ag(1×1)−Au(111) surface, we have used $E_c = 0.45$ V. It should be noted that the shape of the j vs E profile is very similar to those obtained for Ag upd on Au(111) surfaces.[26,27] The inset in Figure 1 also shows that the voltammetric response of our Au(111) substrate in 1 M H_2SO_4 closely resembles those reported on Au(111) single crystals.[36]

The STM image and cross section of the Au(111) surfaces after the underpotential deposition of Ag at $E_c = 0.45$ V is shown in Figure 2. The surface topography is consistent with the Au(111) substrate.[10] Large atomically smooth terraces separated by monatomic height steps are observed without any evidences of three-dimensional Ag clustering, thus supporting the formation of the Ag(1×1)−Au(111) lattice.

The AES spectrum of a Au(111) substrate that has been cycled in 1 M H_2SO_4 and emmersed at $E_c = -0.25$ V is shown in Figure 3a. The Au transitions at 240 eV (N_7VV) are observed together with some C contamination (271 eV, KLL) due to the transfer from the electrochemical cell to the UHV chamber. In principle, the small amount of oxygen (503 eV, KLL) and some traces of sulfur S (152 eV, LMM) could be assigned to some amount of sulfate[37] that could remain adsorbed even at these potential values.

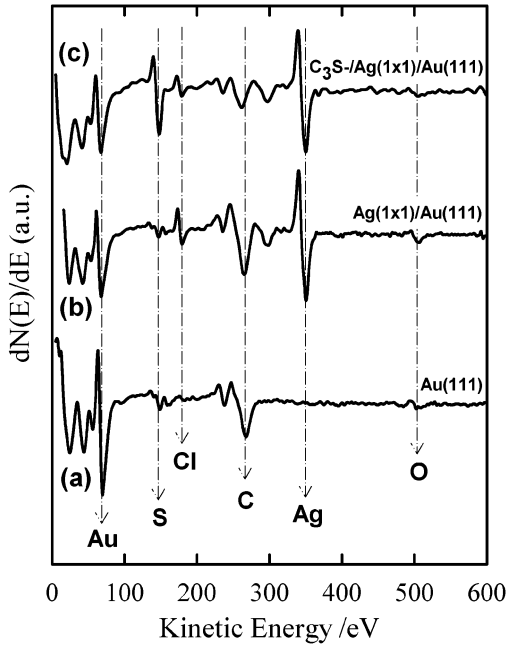

Figure 3. Broad AES spectra for: (a) Au(111) substrate voltammetrically cycled in 1 M H_2SO4 between $E_s = 1.50$ V and $E_c = -0.25$ V, emmersion potential $E_c = -0.25$ V; (b) electrochemically deposited Ag(1×1)−Au(111), emmersion potential $E_c = 0.45$ V; (c) propanethiolate SAM on Ag(1×1)−Au(111) after 20 h in the propanethiol-containing ethanolic solution.

The AES spectrum of the Au(111) substrate after voltammetric deposition of Ag upd followed by emmersion at $E_c = 0.05$ V (Figure 3b) clearly reveals the presence of Ag on the Au surface. In fact, Ag transitions at 352 eV ($M_5N_{4,5}N_{4,5}$) and 357 eV ($M_4N_{4,5}N_{4,5}$) are clearly observed, and accordingly, the intensity of the signal originated in the Au transitions at 70 eV (N_7VV) decreases. The small Cl signal (180 eV, LMM) detected on the upd Ag can be assigned to an enhanced chloride anion adsorption on this surface.[38] Again, the small oxygen and sulfur

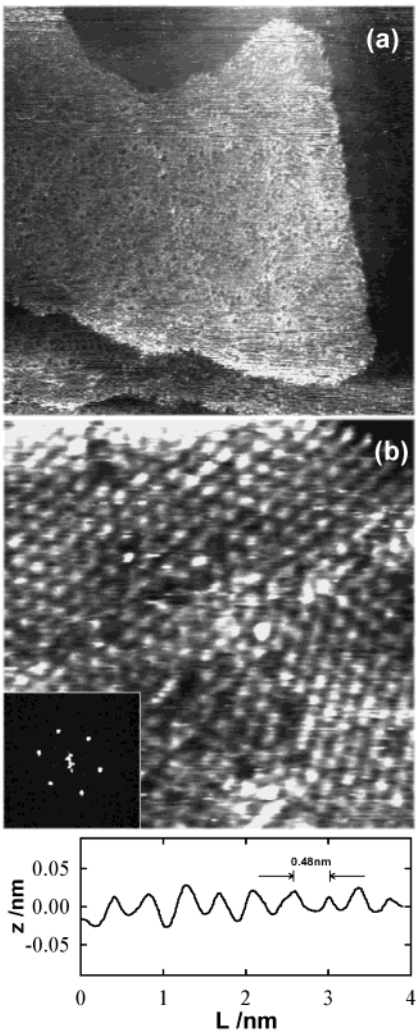

Figure 4. STM images of the propanethiolate SAM on the Ag(1 × 1)−Au(111) surface. (a) 45 × 45 nm^2 image showing atomically smooth terraces and steps; individual molecules can be resolved. (b) 8.5 × 8.5 nm^2 showing the incommesurate adlayer; black holes correspond to vacancies in the SAM. Inset: Fourier transform of the image showing the hexagonal symmetry. (c) Cross section of the STM image showing the nearest-neighbor distance $d = 0.48 \pm 0.03$ nm. Imaging conditions: tunneling voltage $V_t = 650$ mV and tunneling current $I_t = 800$ pA.

signals can be assigned to the sulfate anion adsorption on the Ag(1 × 1) monolayer deposited at upd.[39]

3.2. Preparation and Characterization of the Alkanethiolate SAMs on Ag(1 × 1)−Au(111) Surfaces. After preparation, the upd Ag(1 × 1)−Au(111) surfaces were washed in the sulfuric acid solution, water, and ethanol and finally immersed in the ethanolic solutions containing alkanethiols. After 20 h of immersion, the samples were carefully rinsed with ethanol and dried under nitrogen flux. Afterward, they were imaged by STM. Typical low-resolution images of these surfaces are shown in Figure 4a. The propanethiolate-covered Ag(1 × 1)−Au(111) surface exhibits atomically smooth terraces separated by the monatomic steps. Some monolayer vacancies can be clearly seen at the upper and lower terraces. It has been reported that short-chain alkanethiolate SAMs on Au(111) exhibit a large number of defects at the monolayer.[5b] However, as already reported,[29] large holes corresponding to vacancy gold islands usually observed after alkanethiolate self-assembly on Au(111) and Ag-(111) are not detected in the Ag(1 × 1)−Au(111) surface, i.e., the stability of the Ag surface on Au seems to be increased. It

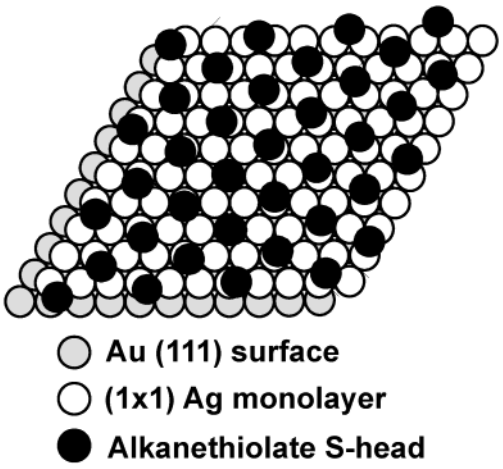

Figure 5. Scheme of the incommensurate alkanethiolate lattice on the Ag(1 × 1)−Au(111) substrate.

should be also noted that no traces of the c(4 × 2) superlattice, usually observed for alkanethiolate self-assembled on the Au-(111) surface, are detected, then confirming that the Au(111) substrate is completely covered by the Ag(1 × 1) lattice. Arrays of molecules are also resolved in Figure 4a. By increasing the STM resolution, we were able to observe ordered domains of a hexagonal lattice (Figure 4b and inset) with nearest-neighbor distances $d = 0.48 \pm 0.03$ nm (Figure 4c) in a very close agreement to that observed for the incommensurate octadecanethiolate lattice on Ag(111)[14] and also close to that reported for butanethiolate adsorption on Ag upd-Au(111).[29] Our d value arises from a rigorous statistical analysis of the nearest-neighbor distances (measured in the fast x-scanning direction to minimize drift effects) from different STM images. It has been reported that short-chain alkanethiolates, including propanethiolate adlayers, form the well-known commensurate ($\sqrt{7} \times \sqrt{7}$)R19.1° lattice (lattice constant 0.44 nm) on Ag(111) surfaces.[40] Our STM results show that the propanethiolate species chemisorb on the Ag(1 × 1)−Au(111) surface forming a incommensurate lattice in a fashion similar to long-chain alkanethiolates on Ag(111),[12a] differing from that observed for propanethiolate on Ag(111). This interesting fact, concerning to the observation of $d = 0.48$ nm, longer than that expected for the ($\sqrt{7} \times \sqrt{7}$)-R19.1° lattice ($d = 0.44$ nm), is reinforced by recent reported STM results on butanethiolate monolayers self-assembled on Ag-upd-modified Au(111) surfaces.[29] On those STM studies it was found that buthanethiolate species organize on the Ag-modified Au(111) surface forming ordered adlayers with $d =$ 0.5 nm. Otherwise, spectroscopic data have shown that the self-assembly of alkanethiolate species on Ag upd on Au(111) results in a surface structure distinct from those found on the Au(111) and Ag(111) surfaces.[32] A scheme of the incommensurate lattice is shown in Figure 5. Vacancies at the propanethiolate SAMs are also evident in the STM images (Figure 4b).

In Figure 3, we also include the broad AES spectrum of the propanethiolate-covered Ag(1 × 1)−Au(111) surface after the self-assembly process (Figure 3c). The presence of the propanethiolate SAMs on the Ag(1 × 1)−Au(111) surface is clearly revealed by the S(LMM) and C(KLL) transitions at 152 and 271 eV, respectively. In this case, the intensity of the C and S signals is consistent with the presence of a propanethiolate monolayer at the surface. Note that the intensity of the Ag signal is similar to that observed for the propanethiolate-free surface (Figure 3b), revealing that the Ag upd layer is not etched during the self-assembly process. The amounts of oxygen and chloride become even smaller than the traces observed on the Ag(1 ×

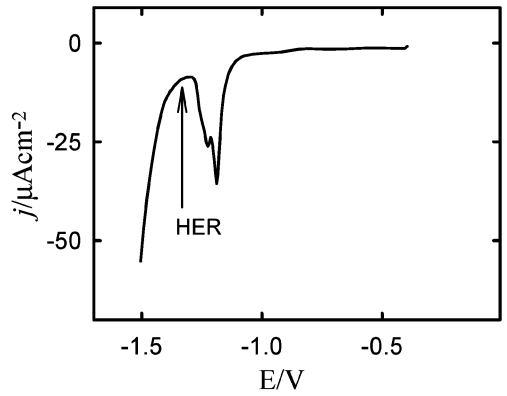

Figure 6. Cathodic polarization curve recorded at 0.05 V s^{-1} for a propanethiolate SAM on Ag(1 × 1)−Au(111). The electrodesorption peak corresponding to the incommensurate lattice stripping from this surface is shown at $E_p = -1.19$ V. The onset of the hydrogen evolution reaction (*HER*) is indicated by an arrow.

1)−Au(111) surface. It means that the traces of adsorbed sulfates and chlorides are displaced by the propanethiolate ions, and adsorbed propanethiolates prevent C contamination during the sample transfer. The negligible oxygen signal also indicates that no significant amounts of Ag oxides remains on the Ag(111) surface after the self-assembly process in the ethanolic solution.[11e]

3.3. Electrodesorption Curves for Alkanethiolate SAMs on Ag(1 × 1)−Au(111) Surfaces. A typical cathodic polarization curve recorded for propanethiolate electrodesorption from the Ag(1 × 1)−Au(111) surface shows a well-defined peak at $E_p = -1.19$ V with a small contribution at the cathodic side (Figure 6). Two peaks have been reported for alkanethiolate electrodesorption from Ag(111), the cathodic one assigned to the desorption of a diluted disordered alkanethiolate phase.[18] However, in our case, this feature can be considered as a peak splitting due to different surface coordination sites[19] involved in the incommesurate lattice rather than two different peaks involving different surface phases. In the case of alkanethiolates with longer hydrocarbon chains, electrodesorption takes place overlapping *HER*. The electrodesorption charge density involved in the electrodesorption curve is ≈ 70 μC cm^{-2}, a figure close to those reported for alkanethiolate SAMs on Au(111) and Ag(111).[16,21]

For $n \leq 10$, E_p shifts linearly in the negative direction as the number of C units in the alkanethiolate molecule increase (Figure 7), whereas for $n > 10$, it remains practically constant.[41] The slope of the E_p vs n plot, which reflects hydrocarbon chain-dependent stabilizing forces at SAMs in aqueous solutions (van der Waals + hydrophobic), is 0.043 V per methylene (∼4 kJ mol^{-1}), close to those obtained for alkanethiolate electrodesorption from Au(111) and Ag(111) (Figure 7). These results for the well-known Ag(111) and Au(111) systems are in excellent agreement with those reported for different authors for these alkanethiolate/metal systems,[15−17] thus supporting the quality of our E_p measurements on the Ag(1 × 1)−Au(111) surface. For $n > 10$, the existence of long-ranged interactions turns E_p values independent of n (Figure 7).[41] Surprinsingly, in the overall n range, E_p values measured on the Ag(1 × 1)−Au(111) surface are shifted by ∼0.10 and 0.40 V in the negative direction with respect to those obtained on Ag(111) and Au(111) surfaces, respectively. This means that alkanethiolate adsorption on the Ag(1 × 1)−Au(111) substrate differs from that expected for adsorption on the Ag(111) and Au(111). In fact, alkanethiolate molecules are more stable on the Ag overlayer on Au(111) than on Ag(111) or on Au(111) surfaces. We note that the E_p value for hexanethiolate electrodesorption from Ag upd over-

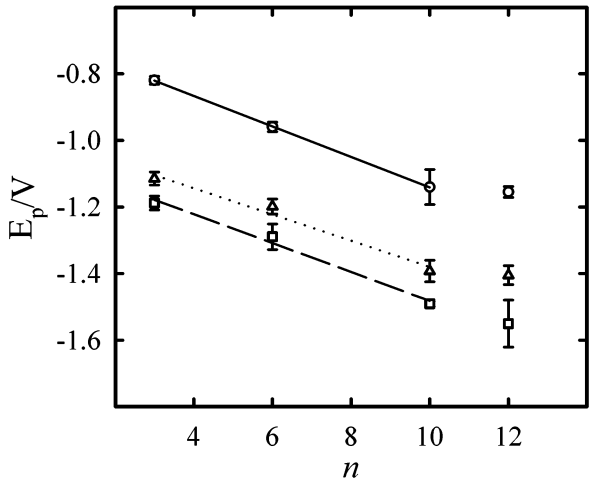

Figure 7. E_p vs n plot for alkanethiolate SAMs electrodesorption from: (□) Ag(1 × 1)−Au(111); (△) Ag(111); and (○) Au(111). The slopes are ∼0.04 V per C unit. Error bars were estimated for a confidence interval of 99%.

layer on Au(111) reported in ref 42 is also shifted in the negative direction when compared to the E_p value reported for hexanethiolate electrodesorption from Ag(111) surfaces.

We have also made electrodesorption runs for propanethiolate SAMs on Ag multilayers deposited on the Au(111) surface and for sub-monolayer Ag coverage ($\theta_{Ag} < 1/3$). In the case of Ag multilayers (more than two silver layers), E_p values agree with those found for propanethiolate electrodesorption from Ag(111) surfaces. It means that the effect of the underlying Au vanishes as the number of Ag layers increases. Conversely for $\theta_{Ag} < 1/3$, a wide electrodesorption peak is observed with E_p values more negative than those measured on Au(111) and more positive than those measured from Ag(111), reflecting the bimetallic nature of the surface. A detailed study for this system will be reported elsewhere.[43]

To elucidate the energetic contributions that stabilize the alkanethiolate SAM on the Ag(1 × 1)−Au(111) surface, we have made DFT calculations for methanethiolate adsorption on a metallic Ag(1×1)−Au(111) cluster.

4. Energetics of the Electrodesorption Process: Quantum DFT Calculations

4.1. Method. Equation 1 involves the introduction of an electron in the alkanethiolate−metal system, the desorption of an alkanethiolate anion, and the solvation of the metal and the alkanethiolate anion. The steps involving in this process can be represented as follows[21]

$$(CH_3)(CH_2)_nS{-}Me + e = [(CH_3)(CH_2)_nS^{-}Me]^- \quad (1a)$$

$$[(CH_3)(CH_2)_nS^{-}Me]^- = (CH_3)(CH_2)_nS^- + Me \quad (1b)$$

$$Me + solvent = Me_{solv} \quad (1c)$$

$$(CH_3)(CH_2)_nS^- + solvent = [(CH_3)(CH_2)_nS^-]_{solv} \quad (1d)$$

where Me represents the metal substrate, the parentheses stand for adsorbed species, and the suffix "solv" indicates a solvated species.

We have evaluated the energetics of steps 1a−c by using DFT calculations following the procedure described in ref 21. DFT calculations are based in the three-parameter hybrid method proposed by Becke, associated with the gradient corrected

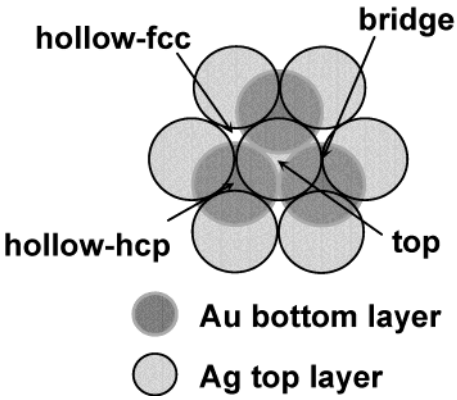

Figure 8. Surface sites of the Ag(1 × 1)−Au(111) cluster model for methanethiolate adsorption as studied by DFT calculations.

correlation functional of Lee, Yang, and Parr, B3LYP.[44] The Ag and Au atoms have been described with 11 electrons, whereas the remainder of the atomic electron density was replaced by relativistic effective core potential (ECP) from Hay and Wadt, LANL1MB.[45] The nd^{10} $(n + 1)s^1$ valence shell, where $n = 4$ (Ag) and $n = 5$ (Au), was treated explicitly with the basis set LANL1MB. S, C, and H atoms are described with the standard 6-31G(d) basis set,[46] which is split valence plus polarization quality. In all cases, the electronic state considered is taken as the lowest-energy closed-shell configuration. The theoretical calculations were performed with the electronic structure software Gaussian 98.[47] We have also calculated the charge remaining in the S atom after methanethiolate adsorption by using Mulliken populations. These are used as a qualitative tool due to their well-known limitations.

The cluster model used to represent the metal surface was built with 10 atoms, 7 in the top layer (Ag) and 3 in the second layer (Au) (Figure 8). The Au−Au and Ag−Ag distances were maintained fixed to the bulk values of 0.2884 and 0.2889 nm, respectively.[48] We have studied four surface sites, hollow hcp, hollow fcc, bridge, and top (Figure 8). Note that hcp and fcc sites involve tetrahedral and octahedral coordination geometries (Figure 8), respectively. The methanethiolate anion was oriented with the sulfur atom oriented toward the metal (Me) surface at a certain distance over the selected surface site. The S−Me distance (d) and the α angle defined between the C−S bond and the substrate normal were optimized, while holding the rest of the anion geometry fixed throughout the calculations, at the optimized values of the isolated anion.

The methanethiolate adsorption energy, E_{ads}, has been defined as

$$E_{ads} = E[Me_{10}SCH_3]^- - [E[Me_{10}] + E[SCH_3^-]] \quad (2)$$

where $E[Me_{10}SCH_3]^-$ is the total energy of $[Me_{10}SCH_3]^-$ with the parameters d and α optimized, $E[Me_{10}]$ is the energy for the 10-atom metal cluster and $E[SCH_3^-]$ is the energy of methanethiolate anion.

The hydration energy of the Au(111), Ag(111), and Ag(1 × 1)−Au(111) surfaces estimated by a 10-atom cluster calculation was performed by using the B3LYP method and employing the 6-31G(d) basis set for the O and H atoms. For the metal atoms, the LANL1MB pseudopotential and basis set were used, as described above. The water molecule was adsorbed at the top position via the oxygen atom; the O−metal distance was optimized in each case, with the molecular plane normal to the metal surface in accordance with what was previously reported in ref 49. The reason for choosing this configuration was due to the well-known fact that water molecules adsorb on a wide range of metal surfaces at the atop position.[50]

TABLE 1: Desorption Energies ($-E_{ads}$), S−Me Bond Length (d), α Value, ϵ_{HOMO}, and Charge on the S Atom for Methanethiolate Adsorbed on the Different Au, Ag, and Ag(1 × 1)−Au(111) Sites

metal cluster	site	d (nm)	α (degrees)	$-E_{ads}$ (kJ mol^{-1})	ϵ_{HOMO} (eV)	charge on the S atom
Au_{10}(111)	hcp	0.227	23.8	246	−1.18	−0.13
	fcc	0.231	58.5	255	−1.08	−0.15
	top	0.260	73.5	209	−1.23	−0.21
	hcp-bridge	0.233	50.5	250	−1.19	−0.16
	fcc-bridge	0.236	30.0	249	−1.22	−0.18
	bridge	0.234	24.9	226	−1.20	−0.18
Ag_{10}(111)	hcp	0.226	33.3	223	−0.53	−0.28
	fcc	0.230	1.96	212	−0.45	−0.28
	top	0.263	68.1	174	−0.54	−0.31
	bridge	0.234	34.8	194	−0.54	−0.29
$Ag_7(1 \times 1)-Au_3$(111)	hcp	0.220	25.4	251	−0.62	−0.27
	fcc	0.221	9.6	247	−0.56	−0.28
	top	0.26	67.1	208	−0.66	−0.27
	bridge	0.228	26.9	237	−0.63	−0.29

TABLE 2: Adsorption Energy of Water on the Different Cluster Models (Top Site)

metal cluster	E_{ads} (kJ mol^{-1})
Ag_{10}(111)	−19.27
Ag_7Au_3(111)	−26.24
Au_{10}(111)	−25.78

4.2. Numerical Results. Results obtained for the methanethiolate anion adsorption on the Ag(1 × 1)−Au(111) surfaces are summarized in Table 1 and compared to those previously reported for methanethiolate adsorption on Au(111) and Ag(111). S−Me bond lengths (d)[5a] and α angles are similar to those calculated for methanethiol adsorption on Ag(111) and Au(111).[51,52] Results also show that the S atom in the C−S−Ag(1 × 1)−Au(111) bond has a negative charge similar to that calculated for the Ag(111) surface.

It has been suggested that the energy to introduce an electron into the methanethiolate/metal system (step 1a) should be related to the work function of the metal surfaces.[19] We have shown that a better correlation is obtained by using the energy (ϵ_{HOMO}) of the highest occupied molecular orbital (HOMO).[21] Note that ϵ_{HOMO} can be considered as a true ionization potential.[53] We have taken the ϵ_{HOMO} values from the DFT calculations as shown in Table 1. These results clearly show that the energy of this step is only slightly higher than that calculated for the Ag(111) but significantly lower than that estimated for the Au(111) surface. It means that from the electronic point of view the Ag(1 × 1)−Au(111) behaves as a Ag(111) surface.

Step 1b involves the desorption energy of the alkanethiolate species. The E_{ads} value increases in the following sequence top < bridge < fcc ≈ hcp. However, the most interesting result shown in Table 1 is that the magnitude of the E_{ads} values for methanethiolate adsorption on the different sites of the Ag(1 × 1)−Au(111) surface is higher than those measured on Ag(111) and close to those calculated on Au(111). It means that the Au second layer strongly modifies the behavior of the Ag layer. This surprinsing result has also been reported for CO adsorption on a monolayer of Pt on top of a Au(111) substrate.[2] This effect has been related to the shift of the d-band center of the metal overlayer. We have also noted that this shift has been reported for the case of a Ag overlayer on Au(111).[3] In the same way, our adsorption data reflect a better interaction between the Ag(1 × 1)−Au(111) surface and the thiolate anion because the

presence of the Ag adlayer raises the Fermi level in relation to the Ag(111) surface. In this sense, the energy of the HOMO for both surfaces are ϵ_{HOMO} Ag(1 × 1)−Au(111) = −3.79 eV and ϵ_{HOMO} Ag(111) = −4.14 eV. The value −3.79 eV for the Ag(1 × 1)−Au(111) is closer to the energy of the high-lying orbital of the isolated thiolate anion (+1.43 eV), allowing a stronger adsorbate−substrate coupling.

The hydration energy estimated by DFT calculations for the adsorption of a water molecule on the Ag(1 × 1)−Au(111) cluster (Table 2) is close to those found for water adsorption on the Au(111) and Ag(111) surfaces.[49]

4.3. Comparative Stability of *n*-Alkanethiolates on the Different Metal Substrates. The energy barrier to desorb an alkanethiolate molecule from the metal surface should involve alkanethiolate−substrate (E_{A-Me}), alkanethiolate−alkanethiolate (E_{A-A}), alkanethiolate−solvent (E_{A-solv}), and substrate−solvent ($E_{Me-solv}$) interaction energies.[21] The energy involved in step 1a (E_{ct}) is related to the energy needed to introduce an electron into the alkanethiolate−metal system.[21] Step 1b involves the desorption energy E_{des}, $E_{des} = -E_{ads}$, that is, *n* independent as already discussed.[5a] Therefore, E_{A-Me} contains both E_{ct} and E_{des}. Step 1b also involves the breaking of hydrocarbon chain−hydrocarbon chain interactions (E_{A-A}). Finally, steps 1c and 1d involve $E_{Me-solv}$ and E_{A-solv}, respectively. The electrodesorption energy (E_{ed}) involved is

$$E_{ed} = E_{des} + E_{A-solv} + E_{A-A} + E_{Me-solv} + E_{ct} \qquad (3)$$

For $n = 0$, the *n*-dependent terms E_{A-solv} and E_{A-A} cancel so that eq 3 becomes

$$E_{ed}^{n=0} = E_{ct} + E_{des} + E_{Me-solv} \qquad (4)$$

To calculate the E_{des} values for alkanethiolate desorption from the Ag(1 × 1)−Au(111), we have averaged E_{des} over all the surface sites due to the incommensurate nature of the adsorbate lattice. For Ag(111) surfaces we have used $E_{des} = (E_{des\ top} + E_{des\ hcp} + E_{des\ fcc})/3$ because the surface structure consists of a (√7 × √7)R19.1° alkanethiolate lattice.[40] On the other hand, to estimate E_{des} for (√3 × √3)R30° alkanethiolate lattice on the Au(111) surface, we have used $E_{des} = E_{des\ hcp} \approx E_{des\ fcc} \approx E_{des\ bridge-hcp} \approx E_{des\ bridge-fcc}$ due to the small differences among the Au(111) substrate sites. A similar procedure has been used to calculate ϵ_{HOMO} for the different surfaces. Therefore we have

Ag(1 × 1)−Au(111)

$$E_{ed}^{n=0} = -59.4\ \text{kJ mol}^{-1} + 235\ \text{kJ mol}^{-1} + (-26.34)\ \text{kJ mol}^{-1} = 149.76\ \text{kJ mol}^{-1}$$

Au(111)

$$E_{ed}^{n=0} = -112.24\ \text{kJ mol}^{-1} + 250\ \text{kJ mol}^{-1} + (-25.78)\ \text{kJ mol}^{-1} = 111.98\ \text{kJ mol}^{-1}$$

Ag(111)

$$E_{ed}^{n=0} = -48.71\ \text{kJ mol}^{-1} + 205\ \text{kJ mol}^{-1} + (-19.27)\ \text{kJ mol}^{-1} = 137.02\ \text{kJ mol}^{-1}$$

It means that $\Delta E_{ed}^{n=0}$ Ag(1 × 1)/Au(111)−Ag(111) = 12.27 kJ mol^{-1} and $\Delta E_{ed}^{n=0}$ Ag(1 × 1)/Au(111)−Au(111) = 37.78 kJ mol^{-1}. Considering a one-electron charge transfer (eq 1), the estimated difference in the peak potential results in $\Delta E_p(n = 0)$ Ag(1 × 1)−Au(111) − Ag(111) = 0.13 V and $\Delta E_p(n = 0)$ Ag(1 × 1)−Au(111) − Au(111) = 0.39 V. These values are in the order of the experimental ΔE_p extrapolated to $n = 0$ (Figure 7): $\Delta E_p(n = 0)$ Ag(1 × 1)−Au(111) − Ag(111) = 0.06 V and $\Delta E_p(n = 0)$ Ag(1 × 1)−Au(111) − Au(111) = 0.36 V.

We have also made calculations in a fixed geometry, using the optimized molecule−surface distance and molecule−surface angle (Table 1), for larger clusters consisting of 18 atoms in the first layer and 10 atoms in the second one. Results obtained with these clusters lead to $\Delta E_p(n = 0)$ Ag(1 × 1)−Au(111) − Ag(111) = 0.08 V and $\Delta E_p(n = 0)$ Ag(1 × 1)−Au(111) − Au(111) = 0.31 V, i.e., very close to those obtained with the 10 atoms clusters. Therefore, it can be concluded that there is no marked cluster size effects on our system. It should be also noted that the adsorption energy for water adsorption on the larger clusters are very similar than those found on the smaller ones. Experimental values for water adsorption on Pt surfaces lead to 30 kJ mol^{-1} values,[54] and it is expected that water adsorption on the other noble metals leads to similar values. In fact, the trend observed in ΔE_p values is the same if the contribution of the water adsorption energy is not included in our calculations.

We have also compared our results from DFT calculations for the 10 atoms cluster model with experimental values for the methanethiolate/Ag(111) interface derived from two-photon photoemission measurements.[55] For this system, it results $\epsilon_{LUMO} - \epsilon_{HOMO} = 3.4$ eV. In fact, we have made Hartree−Fock (HF) calculations for methanethiolate/Ag_{10}(111) sites in the optimized geometry found previously by DFT (Table 1) that lead to an average value $\epsilon_{LUMO} - \epsilon_{HOMO} \approx 3.4$ eV, in excellent agreement with the experimental one. However, our DFT calculations give a smaller difference since it is known that DFT calculations lead to Kohn−Sham orbital energy values that are smaller and scaled by a certain factor with respect to the experimental ones.[56] Nevertheless, we found that the difference between the ϵ_{HOMO} values for methanethiolate/Au_{10}(111) and methanethiolate/Ag_{10}(111) remains the same when they are calculated by DFT or HF. This result validates the use of our cluster model and DFT calculations to estimate *differences* in ϵ_{HOMO} values for the different alkanethiolate metal surfaces.

Despite the fact that the estimated values are in agreement with the experimental ones, we prefer to stress here only some qualitative conclusions derived from these calculations.[3] The unexpected stability of the alkanethiolate Ag(1 × 1)−Au(111) surface arises from a balance between the energy to introduce an electron into the alkanethiolate−Ag(1 × 1)−Au(111) system and the alkanethiolate adsorption energy that is markedly modified by the presence of the Au(111) substrate.

Finally, it can be argued that the electrochemical potential is related to the free energy rather than energy in the enthalpy sense. However, the entropic changes involved in going from ordered alkanethiolate lattices on the different surfaces studied here to solvated alkanethiolates in the solution should be similar. Therefore, entropy contributions should be canceled when considering free energy differences in the reductive electrodesorption taking place from these surfaces.

Conclusions

We have studied the surface structure and electrochemical stability of alkanethiolate SAMs on upd Ag(1 × 1)−Au(111) by using electrochemical techniques, STM imaging, and AES. The Au(111) substrate modifies alkanethiolate adsorption, leading to hexagonal incommensurate surface structures with nearest-neighbor distance (0.48 nm) even for short adsorbed alkanethiolates. For a given alkanethiolate, electrodesorption potentials of the incommensurate alkanethiolate lattice from the Ag(1 × 1)−Au(111) surface are shifted 0.10 and 0.40 V in the negative direction with respect to those determined on Ag(111) and Au(111), respectively. DFT calculations for methanethiolate

desorption from the different surfaces show that the energy to introduce an electron into the alkanethiolate−Ag(1 × 1)−Au(111) system is slightly smaller to that found for the Ag(111) surface. On the other hand, the alkanethiolate desorption energy from the Ag(1 × 1)−Au(111) surface is larger than that found for Ag(111) surfaces and close to that measured for Au(111). The balance between these energies determines the electrodesorption potentials of alkanethiolates from the Ag(1 × 1)−Au(111) surface.

Acknowledgment. This work was supported by the Agencia Nacional de Promoción Científica y Tecnológica (PICT 99-5030) and CONICET (Argentina) and Gobierno Autónomo de Canarias (Project PI2002/034) (Spain).

References and Notes

(1) Gomer, R. *Acc. Chem. Res.* **1996**, *29*, 284.

(2) Pedersen, M. O.; Helveg, S.; Ruban, A.; Stensgaard, I.; Laesgaard, E.; Norskov, J. K.; Besenbacher, F. *Surf. Sci*. **1999**, *426*, 395.

(3) Ruban, A.; Hammer, B.; Stolze, P.; Skriver, H. L.; Norskov, J. K. *J. Mol. Catal. A: Chem.* **1997**, *115*, 421.

(4) Ertl, G. *The Nature of the Surface Chemical Bond*; Rhodin, T. N., Ertl, G., Eds.; North-Holland: New York, 1979.

(5) (a) Ulman, A. *Chem. Rev.* **1996**, *96*, 1533. (b) Finklea, H. O. In *Encycopledia of Analytical Chemistry: Applications, Theory and Instrumentation*; Meyers, R., Ed.; John Wiley & Sons: Chichester, 2000.

(6) Haag, R.; Rampi, A. M.; Holmlin, R. E.; Whitesides, G. M. *J. Am. Chem. Soc.* **1999**, *121*, 7895.

(7) (a) Xia, Y.; Rogers, J. A.; Paul, K. E.; Whitesides, G. M. *Chem. Rev.* **1999**, *99*, 1823. (b) Schilardi, P. L.; Azzaroni, O.; Salvarezza, R. C. *Langmuir* **2001**, *17*, 2747.

(8) Schreiber, F. *Prog. Surf. Sci*. **2000**, *65*, 151 and references therein.

(9) (a) Anselmetti, D.; Baratoff, A.; Guntherodt, H. J.; Delamarche, E.; Michel, B.; Gerber, Ch.; Kang, H.; Wolf, H.; Ringsdorf, H. *Europhys. Lett*. **1994**, *27*, 365. (b) Terán, F. T.; Vela, M. E.; Salvarezza, R. C.; Arvia, A. J. *J. Chem. Phys.* **1998**, *109*, 5703.

(10) (a) Zhong, C.-J.; Brush, R. C.; Anderegg, J.; Porter, M. D. *Langmuir* **1999**, *15*, 518. (b) Vericat, C.; Vela, M. E.; Andreasen, G.; Salvarezza, R. C.; Vázquez, L.; Martín-Gago, J. A. *Langmuir* **2001**, *17*, 4919.

(11) (a) Porter, M. D.; Bright, T. B.; Allara, D. L.; Chidsey, C. E. D. *J. Am. Chem. Soc*. **1987**, *109*, 3559. (b) Nuzzo, R. G.; Dubois, L. H.; Allara, D. L. *J. Am. Chem. Soc*. **1990**, *112*, 558. (c) Bryant, M. A.; Pemberton, J. E. *J. Am. Chem. Soc.* **1991**, *113*, 8284. (d) Hähner, G.; Wöll, C.; Buck, M.; Grunze, M. *Langmuir* **1993**, *9*, 1955. (e) Himmelhaus, M.; Gauss, I.; Buck, M.; Eisert, F.; Wöll, Ch.; Grunze, M. *J. Electron. Spectrosc. Relat. Phenom.* **1998**, *92*, 130.

(12) (a) Nemetz, A.; Fischer, T.; Ulman, A.; Knoll, W. *J. Chem. Phys.* **1993**, *98*, 5912. (b) Dhirani, K. S.; Hines, A.; Fischer, A. J.; Ismail, O.; Guyot-Sionnest, P. *Langmuir* **1995**, *11*, 2609. (c) Fenter, P.; Eisenberg, P.; Li, J.; Camillone, N.; Bernasek, S.; Scoles, G.; Ramanarayanan, T. A.; Liang *Langmuir* **1991**, *7*, 2013.

(13) Aloisi, G. D.; Cavallini, M.; Innocenti, M.; Foresti, M. L.; Pezzatini, G.; Guidelli, R. *J. Phys. Chem. B* **1997**, *101*, 4774.

(14) (a) Fenter, P.; Eisenberger, P.; Li, J.; Camillone, N., III; Bernasek, S.; Scoles, G.; Ramanarayanan, T. A.; Liang, K. S. *Langmuir* **1991**, *7*, 2013. (b) Rieley, H.; Kendall, G. K.; Jones, R. G.; Woodruff, D. P. *Langmuir* **1999**, *15*, 8856.

(15) (a) Widrig, C. A.; Chung, C.; Porter, M. D. *J. Electroanal. Chem.* **1991**, *310*, 335. (b) Walczak, M.; Alves, C. A.; Lamp, B. D.; Porter, M. D. *J. Electroanal. Chem.* **1995**, *396*, 103. (c) Zhong, C.-J.; Porter, M. D. *J. Electroanal. Chem.* **1997**, *425*, 147.

(16) Vela, M. E.; Martin, H.; Vericat, C.; Andreasen, G.; Hernández-Creus, A.; Salvarezza, R. C. *J. Phys. Chem. B* **2000**, *104*, 11878.

(17) Hatchett, D. W.; White, H. S. *J. Phys. Chem.* **1996**, *100*, 9864.

(18) (a) Hatchett, D. W.; Stevenson, K. J.; Lacy, W. B.; Harris, J. M.; White, H. S. *J. Am. Chem. Soc*. **1997** *119*, 6596. (b) Hatchett, D. W.; Uibel, R. H.; Stevenson, K. J.; Harris, J. M.; White, H. S. *J. Am. Chem. Soc.* **1998**, *120*, 1062.

(19) Mohtat, N.; Byloos, M.; Soucy, M.; Morin, S.; Morin, M. *J. Electroanal. Chem*. **2000**, *484*, 120.

(20) Walczak, M. M.; Chung, C.; Stole, S. M.; Widrig, C. A.; Porter, M. D. *J. Am. Chem. Soc.* **1991**, *113*, 2370.

(21) Azzaroni, O.; Vela, M. E.; Andreasen, G.; Carro, P.; Salvarezza, R. C. *J. Phys. Chem. B* **2002**, *106*, 12267.

(22) Palomares, F. J.; Serrano, M.; Ruíz, A.; Soria, F.; Horn, K.; Alonso, M. *Surf. Sci.* **2002**, *513*, 283.

(23) Kolb, D. M. In *Advances in Electrochemistry and Electrochemical Engineering*; Gerischer, H., Tobias, C. W., Eds.; Wiley: New York, 1978; Vol. 11, p 125.

(24) Budevski, E.; Staikov, G.; Lorentz, W. J. *Electrochemical Phase Formation and Growth*; VCH: Weinheim, 1996; Chapter 3.

(25) Adzic, R. R. In *Advances in Electrochemistry and Electrochemical Engineering*; Gerischer, H., Tobias, C. W., Eds.; Wiley: New York, 1985; Vol. 13, p 159.

(26) Esplandiu, M. J.; Kolb, D. M. *Phys. Chem. Chem. Phys.* **1999**, *1*, 4847.

(27) Rooryck, V.; Reniers, F.; Buess-Herman, C.; Attard, G. A.; Yang, X. *J. Electroanal. Chem.* **2000**, *482*, 93 and references therein.

(28) Sánchez, C. G.; Dassie, S. A.; Leiva, E. *Langmuir* **2002**, *18*, 6628.

(29) Hsieh, M.; Chen, Ch. *Langmuir* **2000**, *16*, 1729.

(30) Oyamatsu, D.; Nishizawa, M.; Kuwabata, S.; Yoneyama, H. *Langmuir* **1998**, *14*, 3298.

(31) Jennings, G. K.; Laibinis, P. E. *Langmuir* **1996**, *12*, 6173.

(32) Jennings, G. K.; Laibinis, P. E. *J. Am. Chem. Soc.* **1997**, *119*, 5208.

(33) Oyamatsu, D.; Kanemoto, H.; Kuwabata, S.; Yoneyama, H. *J. Electroanal. Chem.* **2001**, *497*, 97.

(34) Shimazu, K.; Kawaguchi, T.; Isomura, T. *J. Am. Chem. Soc.* **2002**, *124*, 652.

(35) Nishizawa, M.; Sunagawa, T.; Yoneyama, H. *Langmuir* **1997**, *13*, 5215.

(36) Kolb, D. M. In *Structure of Electrified Interfaces*; Lipkowski, J., Ross, P. N., Eds.; VCH Wiley Publishers: New York, 1993; Chapter 3, p 65.

(37) Dretschkow, Th.; Wandlowski, Th. *Ber. Bunsen-Ges. Phys. Chem.* **1997**, *101*, 749.

(38) Michalitsch, R.; Laibinis, P. E. *Angew. Chem., Int. Ed*. **2001**, *113*, 967.

(39) Mrozek, P.; Sung, Y.; Han, M.; Gamboa-Aldeco, M.; Wieckowski, A.; Chen, Ch.; Gewirth, A. *Electrochim. Acta* **1995**, *40*, 17−28.

(40) Heinz, R.; Rabe, J. P. *Langmuir* **1995**, *11*, 506.

(41) Kakiuchi, T.; Usui, H.; Hobara, D.; Yamamoto, M. *Langmuir* **2002**, *18*, 5231.

(42) Esplandiu, M. J.; Hagenströmg, H. *Solid State Ionics* **2002**, *150*, 39.

(43) Fonticelli, M.; Benítez, G.; Azzaroni, O.; Carro, P.; Salvarezza, R. C. In preparation.

(44) Becke, A. D. *J. Chem. Phys.* **1993**, *98*, 5648.

(45) Hay, P.; Wadt, R. *J. Chem. Phys.* **1985**, *82*, 299.

(46) Levine, I. N. *Quantum Chemistry*, 5th ed.; Prentice Hall: New Jersey, 2000; p 492.

(47) Frisch, M. J.; Trucks, G. W.; Schlegel, H. B.; Scuseria, G. E.; Robb, M. A.; Cheeseman, J. R.; Zakrzewski, V. G.; Montgomery, J. A., Jr.; Stratmann, R. E.; Burant, J. C.; Dapprich, S.; Millam, J. M.; Daniels, A. D.; Kudin, K. N.; Strain, M. C.; Farkas, O.; Tomasi, J.; Barone, V.; Cossi, M.; Cammi, R.; Mennucci, B.; Pomelli, C.; Adamo, C.; Clifford, S.; Ochterski, J.; Petersson, G. A.; Ayala, P. Y.; Cui, Q.; Morokuma, K.; Malick, D. K.; Rabuck, A. D.; Raghavachari, K.; Foresman, J. B.; Cioslowski, J.; Ortiz, J. V.; Stefanov, B. B.; Liu, G.; Liashenko, A.; Piskorz, P.; Komaromi, I.; Gomperts, R.; Martin, R. L.; Fox, D. J.; Keith, T.; Al-Laham, M. A.; Peng, C. Y.; Nanayakkara, A.; Gonzalez, C.; Challacombe, M.; Gill, P. M. W.; Johnson, B. G.; Chen, W.; Wong, M. W.; Andres, J. L.; Head-Gordon, M.; Replogle, E. S.; Pople, J. A. Gaussian 98; Gaussian, Inc.: Pittsburgh, PA, 1998.

(48) Kittel, C. *Introduction to Solid State Physics*, 6th ed.; Wiley: New York, 1966.

(49) Kuznetsov, A. M.; Maslii, A. N.; Shapnik, M. S. *Russ. J. Electrochem.* **2000**, *36*, 1309.

(50) Berkowitz, M. L.; Yeh, I.-C.; Spohr, E. In *Interfacial Electrochemistry: Theory, Experiments and Applications*; Wieckowski, A., Ed.; Marcel Dekker: New York, 1999; Chapter 3, p 33.

(51) Akinaga, Y.; Najajima, T.; Hirao, K. *J. Chem. Phys.* **2001**, *114*, 8555.

(52) Gottschalck, J.; Hammer, B. *J. Chem. Phys.* **2002**, *116*, 784.

(53) Chong, D. P.; Gritsenko, O. V.; Baerends, E. J. *J. Chem. Phys.* **2002**, *116*, 1760.

(54) (a) Pirug, G.; Bonzel, H. P. In *Interfacial Electrochemistry: Theory, Experiments and Applications*; Wieckowski, A., Ed.; Marcel Dekker: New York, 1999; Chapter 16, p 269. (b) Thiel, P. S.; Madey, T. E. *Surf. Sci. Rep.* **1987**, *7*, 211.

(55) Miller, A. D.; Gaffney, K. J.; Liu, H. S.; Szymanski, P.; Garret-Roe, S.; Wong, C. M.; Harris, C. B. *J. Phys. Chem. A* **2002**, *106*, 7636.

(56) Stowasser, R.; Hoffmann, R. *J. Am. Chem. Soc.* **1999**, *121*, 3414.